

**Atmospheric mercury sources in a coastal-urban environment: A
case study in Boston, Massachusetts, USA.**

Supplementary Information

S1. Model parameterization

Chemical loss in the box, L_{ox} , is calculated at each time step as follows:

$$L_{ox} = k_L \times C_{box} \times h \times l \times L \quad \text{Eq. S1}$$

where k_L is a rate constant calculated as the inverse of the lifetime of GEM against oxidation in the atmosphere (1) (see Table S2), C_{box} the GEM concentration in the box, h the boundary layer height, and $l \times L$ the area of the box.

The amount of GEM removed via dry deposition is calculated according to Eq. S2:

$$D_{deposition} = v_{deposition} \times C_{box} \times l \times L \quad \text{Eq. S2}$$

where $v_{deposition}$ is the dry deposition velocity of GEM over a mixed urban/forested area (in m/h) (2) (see Table S2).

E_{soil} was calculated using the procedure outlined by Khan et al.(3). Based on flux measurements, Khan et al. proposed the following parameterization:

$$E_{soil} = 10^{0.709 + 0.119 \log(C_{soil}) + 0.137 \log(R_g)} \frac{1}{a} \sin \frac{\pi n}{d} \quad \text{Eq. S3}$$

where C_{soil} is the concentration of legacy Hg in soils (in $\mu\text{g/g}$) according to Eckley et al.(4) (see Table S2), a a constant (see Table S2), d the duration between sunrise and sunset, and n the time of daylight hours which have passed at the time at which emissions are being calculated ($n=0$ at night). R_g is a factor calculated as follows:

$$R_g = SWR e^{-\alpha LAI} \quad \text{Eq. S4}$$

where SWR is the amount of downward shortwave radiation, α a constant (see Table S2), and LAI the leaf area index.

The flux out of the box is calculated according to Eq. S5, where w is the wind speed:

$$F_{out} = C_{box} \times w \times h \times L \quad \text{Eq. S5}$$

The amount of GEM lost to deposition per unit area of ocean, D_{ocean} , is calculated according to Eq. S6, where v_{ocean} is the deposition velocity over open water (in m/h, see Table S2) (2) and C_{ocean} the GEM concentration over the ocean.

$$D_{ocean} = v_{ocean} \times C_{ocean} \quad \text{Eq. S6}$$

Chemical loss over the ocean, L_{ocean} , is calculated as follows:

$$L_{ocean} = k_L \times C_{ocean} \quad \text{Eq. S7}$$

S2. Sensitivity analysis

Two months were identified as periods of potential interest for the purpose of examining the sensitivity of the model: January and August. These two months were selected primarily in order to test the sensitivity of the model in both the warm summer months and cold winter months, when different pathways in the cycle of Hg are enhanced or dampened. In addition, January and August contained several alternating periods of high and low GEM concentrations with no direct correlation with CO₂ and CH₄ indicating variation in wind direction and likely source input over the month. The analysis of back trajectories confirmed that January and August were subject to input of air parcels from several alternating directions and locations (not shown), making them excellent candidates for analyzing model sensitivity to the full range of input variables.

To perform the sensitivity analysis, a reference run was conducted using the assumed variable values taken from the literature (see Table S2). Then, sensitivity runs were conducted by varying each variable, one at a time by $\pm 25\%$. The average percent change in the output GEM concentration from the reference run concentration due to changing a given variable by $\pm 25\%$ is reported for each variable in Table S3. The box model was largely insensitive to changes in most input variables. The exception to this is $C_{land\ in}$, the GEM concentration measured at Harvard Forest used to calculate the flux into the western side of the box. Changing this variable by $\pm 25\%$ led to changes in the output GEM concentration of nearly the same magnitude. The Tekran instrument used to record GEM concentrations at Harvard Forest has an uncertainty of $\pm 10\%$ (5). Further, $C_{land\ in}$ was calculated on a monthly basis from the mean of the Harvard Forest measurements. The standard deviation in each monthly dataseries ranged from 10-15% of the mean. Thus, 25% was taken to represent a reasonable upper bound on the potential error in $C_{land\ in}$, and the main likely source of error in the box model results. All error ranges in model outputs were thus calculated by varying $C_{land\ in}$ by $\pm 25\%$ and recording the corresponding change in model output as the upper or lower bound.

S3. Long range transport from other states

In order to identify potential source regions of GEM, we performed a Potential Source Contribution Function (PSCF) analysis – commonly used in the literature (e.g., 6–10) – using the *trajLevel* function in R package *openair* (11). Based on air-mass back trajectories (see below) and GEM concentrations measured at BU, the PSCF calculates the probability that a source is located at latitude i and longitude j . PSCF solves:

$$PSCF = m_{ij} / n_{ij} \quad \text{Eq. S8}$$

where n_{ij} is the number of times that the trajectories passed through the cell (i, j) and m_{ij} the number of trajectories passing through that cell in which the GEM concentration was greater than the median concentration during the entire study period. Note that cells with few data have a weighting factor applied to reduce their effect (10).

HYSPLIT (12) (HYbrid Single Particle Lagrangian Integrated Trajectory) 24-hour air-mass back trajectories used in the PSCF analysis were generated using the high resolution (12 km) meteorological data produced by the North American Mesoscale Forecast System (NAM) weather forecast model. As shown in Fig. S4, the probability of an anthropogenic source located outside Massachusetts and regularly impacting GEM measurements at BU is low. The oceanic source that can be identified in this analysis is further investigated and discussed in Section 3.3 of the main manuscript.

Table S1: Atmospheric Mercury Network (AMNet) site locations and general description, after Gay et al.(13).

Site ID	Site Name	Location	Latitude	Longitude	Elevation (m)	Data used
AK03	Denali National Park	remote	63.7232	-148.9676	661	Mar-14 to Oct-18
AL19	Birmingham	urban	33.553	-86.8148	177	Jan-09 to Jun-16
FL96	Pensacola	rural	30.55	-87.3753	44	Jan-09 to Nov-16
GA40	Yorkville	rural	33.9283	-85.0456	394	Jan-09 to Oct-16
HI00	Mauna Loa	high altitude	19.5362	-155.5761	3384	Dec-10 to Dec-18
MD08	Piney Reservoir	rural	39.7054	-79.0126	761	Jan-09 to Jul-17
MS12	Grand Bay NERR	rural	30.4124	-88.4038	1	Jan-09 to Oct-17
NJ30	New Brunswick	urban	40.4728	-74.4224	21	Oct-16 to Dec-17
NS01	Kejimkujik	rural	44.4312	-65.2031	158	Jan-09 to Dec-17
NY06	New York City	urban	40.8679	-73.8782	26	Aug-08 to Dec-17
OH02	Athens	rural	39.308	-82.1182	274	Jan-09 to Dec-17
UT97	Salt Lake City	urban	40.7118	-111.9612	1099	Dec-08 to Aug-17
VT99	Underhill	rural	44.5285	-72.8682	397	Jan-09 to Jan-16
WI07	Horicon	rural	43.4557	-88.6169	272	Jan-11 to Dec-17

Table S2: Summary of all variables and their values used in the one-box model.

Variable	Name	Value	Unit	Source
a	Soil constant	1.5	-	Khan et al.(3)
α	Extinction coefficient	0.5	-	Khan et al.(3)
$C_{land\ in}$	Land GEM concentration	Variable	ng/m ³	Harvard Forest monitoring data (see Section 2.2)
C_{soil}	GEM soil concentration	0.088	μg/g	Eckley et al.(4)
d	Number of daylight hours	Variable	-	-
E_{NEI}	Anthropogenic emission rate (prior)	4.19	ng/m ² /h	2014 National Emission Inventory(14)
E_{ocean}	Ocean emission rate (prior)	Variable	ng/m ² /h	MITgcm model(15)
h	Boundary layer height	Variable	m	HRRR model(16)
k_L	Oxidation rate	0.00051	h ⁻¹	Horowitz et al.(1)
LAI	Leaf area index	Variable	m ² /m ²	MODIS-Terra(17)
n	Hours of daylight	Variable	-	-
$S = l \times L$	Area of the box	55660 × 51296	m ²	GMAO 0.5°x0.625° grid(18)
SWR	Shortwave radiation	Variable	W/m ²	HRRR model(16)
v_{ocean}	Ocean deposition rate	0.01	cm/s	Zhang et al.(2)
$v_{deposition}$	Deposition velocity over land	0.1	cm/s	Zhang et al.(2)
w	Wind speed	Variable	m/h	HRRR model(16)

Table S3: Results of the sensitivity analysis conducted for the box model. The values reported are the percent changes in the model output GEM concentration from a reference run due to changing the given variable by $\pm 25\%$ when running the model for the given month. The reference run for the given month was conducted with all variables set to their assumed values (see Table S2).

Variable	January +25%	January -25%	August +25%	August -25%
a	-0.16	0.26	-0.57	0.93
α	-0.01	0.01	-0.09	0.09
$C_{land\ in}$	18.86	-18.66	13.36	-13.50
C_{soil}	0.05	-0.06	0.18	-0.22
E_{NEI}	2.95	-3.16	4.15	-4.28
E_{ocean}	1.07	-1.04	2.38	-2.38
h	-0.95	1.53	-1.01	1.86
k_L	-0.48	0.50	-0.82	0.85
LAI	-0.01	0.01	-0.09	0.09
SWR	0.06	-0.07	0.21	-0.25
v_{ocean}	-1.28	1.59	-3.15	3.83
$v_{deposition}$	-1.67	1.69	-2.48	2.59
w	-1.20	1.83	-1.73	2.77

Table S4: Correlation coefficients and residual values calculated between observations and the model estimates using prior and adjusted emissions.

	Prior emissions		Adjusted emissions	
	R ²	Residual (%)	R ²	Residual (%)
January	-0.30	27	0.87	11
February	-0.25	47	0.77	15
March	0.15	39	0.77	19
April	-0.33	25	0.72	8
May	0.14	31	0.53	11
June	0.22	22	0.19	10
July	0.09	33	0.24	16
August	0.34	30	0.52	13
September	-0.41	39	0.20	21
October	0.50	21	0.59	11
November	0.46	21	0.70	10
December	0.25	21	0.72	8

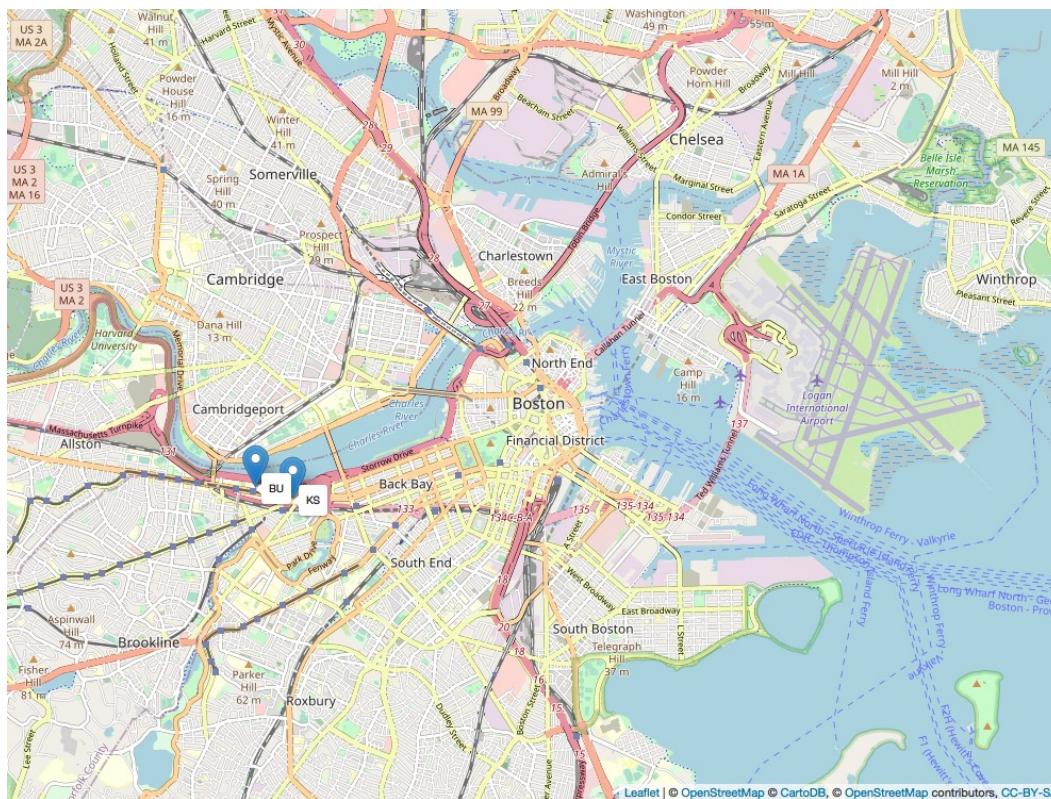


Figure S1: Location of the monitoring sites. Hg in ambient air was monitored at Boston University (BU) while ancillary parameters were monitored at BU (CO₂ and CH₄) and Kenmore Square (KS) station (SO₂). This Figure was made using R package leaflet (19).

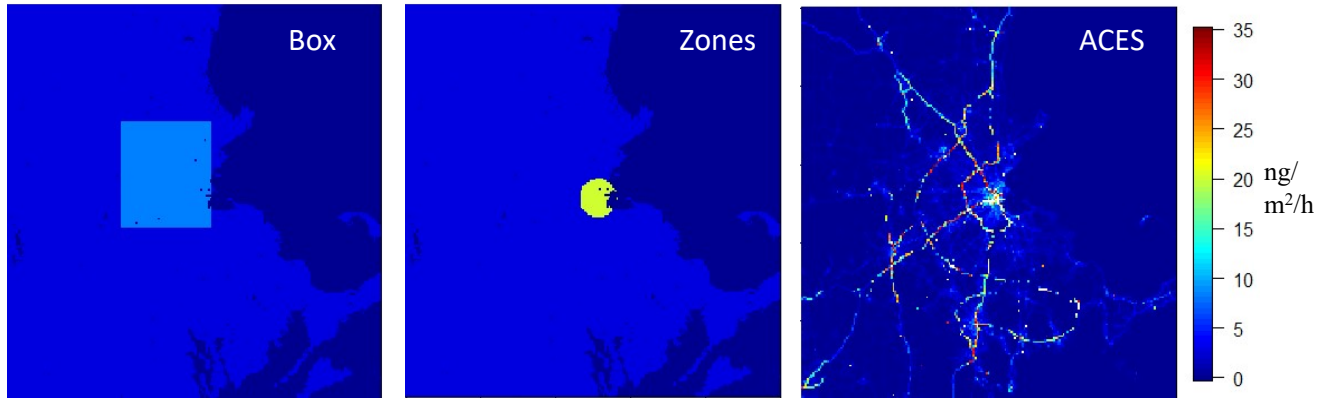


Figure S2: Prior emissions used with the HYSPLIT model. Left: “Box” corresponds to the box model analysis. Center: “Zones” - 20 $\text{ng}/\text{m}^2/\text{h}$ within 10 km of Boston, 3 $\text{ng}/\text{m}^2/\text{h}$ elsewhere. Right: “ACES” – ACES CO_2 emissions scaled to match NEI 2014 totals.

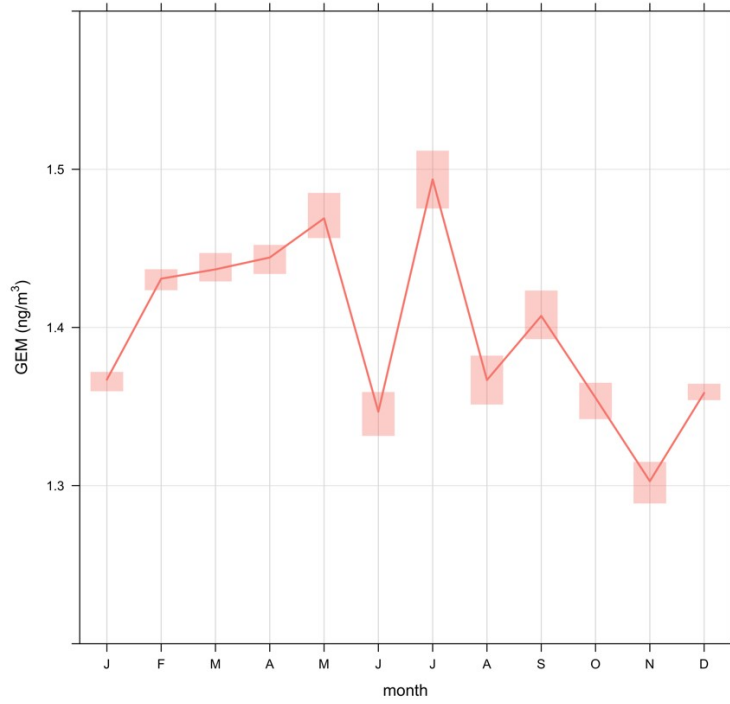


Figure S3: Mean seasonal variation of GEM concentrations at the BU site along with the 95% confidence interval in the mean.

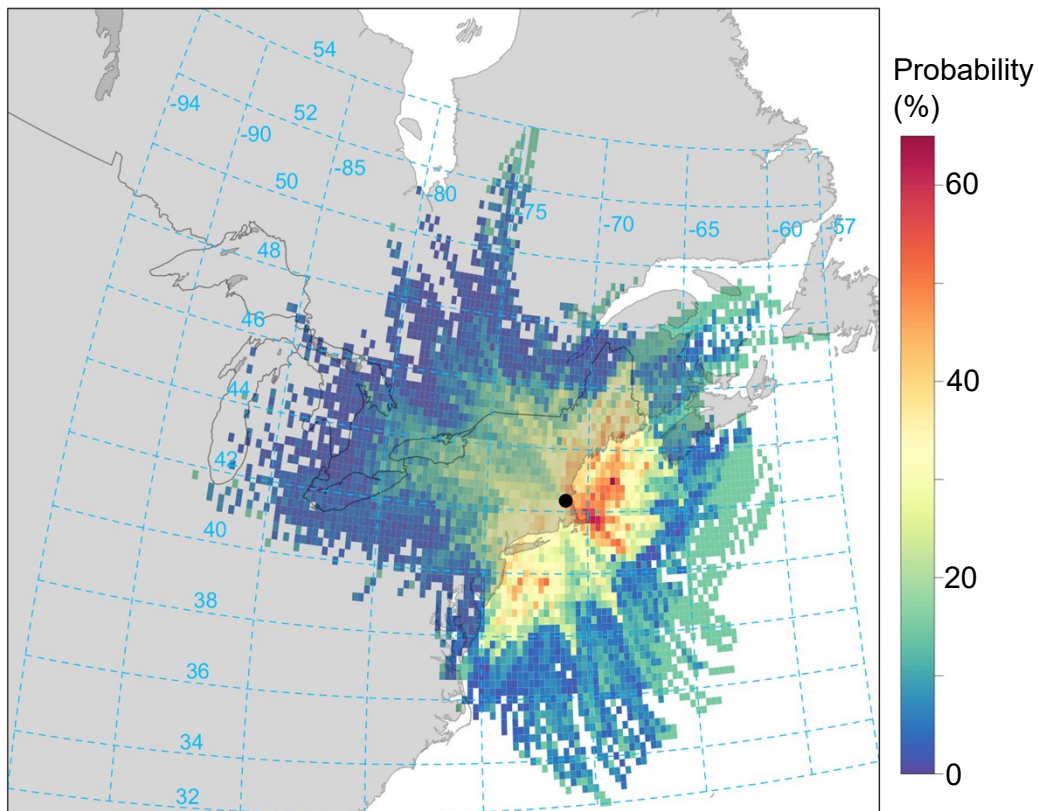


Figure S4: Potential Source Contribution Function (PSCF) analysis based on hourly 24-hour back-trajectories generated with HYSPLIT. This Figure shows the probability of measuring at BU (black dot) a GEM concentration higher than the median over the full study period.

References

1. Horowitz HM, Jacob DJ, Zhang Y, Dibble TS, Slemr F, Amos HM, et al. A new mechanism for atmospheric mercury redox chemistry: implications for the global mercury budget. *Atmos Chem Phys*. 2017 May 29;17(10):6353–71.
2. Zhang L, Wright LP, Blanchard P. A review of current knowledge concerning dry deposition of atmospheric mercury. *Atmospheric Environment*. 2009 Dec; 43(37):5853–64.
3. Khan TR, Obrist D, Agnan Y, Selin NE, Perlinger JA. Atmosphere-terrestrial exchange of gaseous elemental mercury: parameterization improvement through direct comparison with measured ecosystem fluxes. *Environ Sci: Processes Impacts*. 2019 Oct 16;21(10):1699–712.
4. Eckley CS, Tate MT, Lin C-J, Gustin M, Dent S, Eagles-Smith C, et al. Surface-air mercury fluxes across Western North America: A synthesis of spatial trends and controlling variables. *Science of The Total Environment*. 2016 Oct 15; 568:651–65.
5. Slemr F, Angot H, Dommergue A, Magand O, Barret M, Weigelt A, et al. Comparison of mercury concentrations measured at several sites in the Southern Hemisphere. *Atmos Chem Phys*. 2015 Mar 19; 15(6):3125–33.
6. Choi H-D, Holsen TM, Hopke PK. Atmospheric Mercury (Hg) in the Adirondacks: Concentrations and Sources. *Environ Sci Technol*. 2008 Aug 1; 42(15):5644–53.
7. Diéguez MC, Bencardino M, Garcia PE, D'Amore F, Castagna J, De Simone F, et al. A multi-year record of atmospheric mercury species at a background mountain station in Andean Patagonia (Argentina): Temporal trends and meteorological influence. *Atmospheric Environment*. 2019 Jul 3;116819.
8. Duan L, Wang X, Wang D, Duan Y, Cheng N, Xiu G. Atmospheric mercury speciation in Shanghai, China. *Science of The Total Environment*. 2017 Feb 1; 578:460–8.
9. Fu XW, Feng X, Liang P, Deliger, Zhang H, Ji J, et al. Temporal trend and sources of speciated atmospheric mercury at Waliguan GAW station, Northwestern China. *Atmos Chem Phys*. 2012 Feb 20;12(4):1951–64.
10. Han Y-J, Holsen TM, Hopke PK, Yi S-M. Comparison between Back-Trajectory Based Modeling and Lagrangian Backward Dispersion Modeling for Locating Sources of Reactive Gaseous Mercury. *Environ Sci Technol*. 2005 Mar 1;39(6):1715–23.
11. Carslaw D, Ropkins K. openair - An R package for air quality data analysis. *Environ Modell Softw*. 2012 Jan;27–28:52–61.
12. Stein AF, Draxler RR, Rolph GD, Stunder BJB, Cohen MD, Ngan F. NOAA's HYSPLIT Atmospheric Transport and Dispersion Modeling System. *Bull Amer Meteor Soc*. 2015 May 4;96(12):2059–77.
13. Gay DA, Schmeltz D, Prestbo E, Olson M, Sharac T, Tordon R. The Atmospheric Mercury Network: measurement and initial examination of an ongoing atmospheric mercury record across North America. *Atmos Chem Phys*. 2013 Nov 22;13(22):11339–49.

14. US EPA. 2014 National Emissions Inventory (NEI) Data [Internet]. US EPA. 2016 [cited 2019 Aug 9]. Available from: <https://www.epa.gov/air-emissions-inventories/2014-national-emissions-inventory-nei-data>
15. Zhang Y, Jacob DJ, Dutkiewicz S, Amos HM, Long MS, Sunderland EM. Biogeochemical drivers of the fate of riverine mercury discharged to the global and Arctic oceans. *Global biogeochemical cycles*. 2015;29.
16. Benjamin SG, Weygandt SS, Brown JM, Hu M, Alexander CR, Smirnova TG, et al. A North American Hourly Assimilation and Model Forecast Cycle: The Rapid Refresh. *Mon Wea Rev*. 2015 Dec 21;144(4):1669–94.
17. Leaf Area Index (1 month - Terra/MODIS) | NASA [Internet]. Leaf Area Index (1 month - Terra/MODIS) | NASA. 2019 [cited 2019 Aug 9]. Available from: https://neo.sci.gsfc.nasa.gov/view.php?datasetId=MOD15A2_M_LAI
18. GEOS-Chem horizontal grids - Geos-chem [Internet]. [cited 2019 Aug 9]. Available from: http://wiki.seas.harvard.edu/geos-chem/index.php/GEOS-Chem_horizontal_grids#0.5_x_0.625_NA_nested_grid
19. Graul C. leafletR: Interactive Web-Maps Based on the Leaflet JavaScript Library [Internet]. 2016. Available from: <http://cran.r-project.org/package=leafletR>